The Canadian Mineralogist
Vol. 32, pp. 387-396 (1994)

STRUCTURE AND HYDROGEN BONDING IN PREOBRAZHENSKITE, A COMPLEX HETEROPOLYHEDRAL BORATE

PETER C. BURNS AND FRANK C. HAWTHORNE

Department of Geological Sciences, University of Manitoba, Winnipeg, Manitoba R3T 2N2

ABSTRACT

The crystal structure of preobrazhenskite, $Mg_3[B_{11}O_{15}(OH)_9]$, orthorhombic, *a* 16.291(4), *b* 9.181(2), *c* 10.571(2) Å, *V* 1581.3(6) Å^3, *Z* = 4, space group *Pbcn*, has been refined by full-matrix least-squares methods to an *R* index of 4.0% and a *wR* index of 4.1% for 2094 unique observed [$I \geq 2.5\sigma(I)$] reflections measured with Mo*K*α X-radiation. The preobrazhenskite structure contains a 9:(4Δ + 5*T*) + 2*T* fundamental building block (*FBB*), which is the third largest *FBB* known in a borate mineral. Each *FBB* contains four three-membered boron–oxygen rings, each of which is (1Δ + 2*T*). The *FBB*s corner-share with four other *FBB*s, forming complex borate sheets that run parallel to (010). The two Mg positions are located between the borate sheets; both atoms are in octahedral coordination, and each octahedral ligand is also part of the borate sheets, providing strong intersheet bonding through the Mg positions. Hydrogen bonding plays three structural roles: (1) a symmetrical hydrogen-bond occurs within the *FBB*; (2) hydrogen bonds bridge anions of the same borate sheets (but between different *FBB*s); (3) hydrogen bonds bridge adjacent borate sheets. The powder infrared spectrum of preobrazhenskite in the principal OH-stretching region contains five bands corresponding to the five distinct hydrogen positions. The band frequencies in this region are a linear function of the bond-valence deficiency at the acceptor anions, and the intensities of the bands are strongly a function of bond energy.

Keywords: preobrazhenskite, borate, structure refinement, hydrogen bonding, crystal structure, infrared spectroscopy.

SOMMAIRE

La structure cristalline de la préobrazhenskite, $Mg_3[B_{11}O_{15}(OH)_9]$, orthorhombique, *a* 16.291(4), *b* 9.181(2), *c* 10.571(2) Å, *V* 1581.3(6) Å^3, *Z* = 4, groupe spatial *Pbcn*, a été affinée par moindres carrés à matrice entière jusqu'à un résidu *R* de 4.0% (*wR* = 4.1%) en utilisant 2094 réflexions uniques observées [$I \geq 2.5\sigma(I)$] et mesurées avec rayonnement Mo*K*α. La structure de ce minéral contient une trame fondamentale (TF) de type 9:(4Δ + 5*T*) + 2*T*, ce qui serait la troisième unité de base la plus volumineuse que l'on connaisse dans un borate. Chaque TF contient quatre anneaux à trois groupes bore–oxygène, dont chacun est (1Δ + 2*T*). Les TF sont articulés avec quatre autres TF par partage de coins, et l'ensemble forme ainsi des feuillets de borate complexes parallèles à (010). Les deux positions des atomes Mg sont situées entre les feuillets de borate. Dans chaque cas, il s'agit d'une coordinence octaédrique; chaque ligand octaédrique fait aussi partie du feuillet de borate, et produit une forte liaison inter-feuillet par l'intermédiaire des atomes de Mg. Les liaisons hydrogène jouent trois roles structuraux: 1) une liaison hydrogène symétrique caractérise chaque TF, 2) des liaisons hydrogène assurent la liaison entre anions au sein d'un même feuillet de borate, mais entre des TF distinctes, et 3) d'autres agissent comme liaisons entre feuillets de borate adjacents. Le spectre d'absorption infra-rouge obtenu sur poudre dans la région de l'étirement dû aux groupes OH contient cinq bandes correspondant aux cinq positions distinctes de l'hydrogène. Les fréquences observées dans cette région sont une fonction linéaire de la déficience en valences de liaison des anions récepteurs, et les intensités des bandes dépendent fortement de l'énergie des liaisons.

(Traduit par la Rédaction)

Mots-clés: préobrazhenskite, borate, affinement de la structure, liaisons hydrogène, structure cristalline, spectroscopie infra-rouge.

INTRODUCTION

Preobrazhenskite, $Mg_3[B_{11}O_{15}(OH)_9]$, has been found only in the Inder borate deposits of western Kazakhstan. It occurs in small amounts throughout the saliferous strata, where it is associated with halite, polyhalite, kaliborite, boracite and inyoite (Yarzhemskii 1956). Rumanova *et al.* (1972) refined the structure of preobrazhenskite to an *R* index of 18.3% using photographic X-ray data. The precision of their data precluded location of the hydrogen atoms; as a result, the nature of the hydrogen bonding in the structure is not clear (Clark & Christ 1977).

Preobrazhenskite contains one of the largest *FBB*s

(fundamental building blocks) observed in a borate structure. Such large *FBB*s may polymerize to form zeolite-like borate frameworks, such as recently observed in the polymorphs pringleite and ruitenbergite (Grice *et al.* 1994). The study of borates with large *FBB*s is of considerable interest, both in terms of understanding the complex polyanions that form them, and in predicting the types of frameworks that they may produce if combined together. Here we report a refinement of the structure of preobrazhenskite and the precise nature of the *FBB* and the hydrogen bonding contained therein.

Experimental

Collection of X-ray data

A crystal of preobrazhenskite from the Inder borate deposit, Kazakhstan, was ground to an ellipsoidal shape and mounted on a Nicolet *R*3*m* automated four-circle diffractometer. Twenty-five reflections over the range $8° \le 2\theta \le 48°$ were centered using graphite-monochromated Mo$K\alpha$ X-radiation. The unit-cell dimensions (Table 1) were derived by least-squares refinement from the setting angles of the twenty-five automatically aligned reflections. A total of 2645 reflections was measured over the range $4° \le 2\theta \le 60°$, with indices covering the range $0 \le h \le 22$, $0 \le k \le 12$, $0 \le l \le 14$. Two standard reflections were measured every fifty reflections; no significant change in their net intensities occurred during data collection. An empirical absorption correction based on 36 psi-scans for each of 11 reflections over the range $11° \le 2\theta \le 56°$ was applied, reducing *R*(azimuthal) from 2.0 to 1.4%. The data were corrected for Lorentz, polarization and background effects; of the 2645 reflections measured, there were 2094 unique observed [$I \le 2.5\sigma(I)$] reflections.

TABLE 1. MISCELLANEOUS INFORMATION FOR PREOBRAZHENSKITE

Space group	*Pbcn*	Crystal Size (mm)	0.30x0.30
a(Å)	16.291(4)		x0.50
b(Å)	9.181(2)	Total Ref.	2645
c(Å)	10.571(2)	[$I \ge 2.5\sigma$ (I)]	2094
V(Å^3)	1581.3(6)	Final *R*	4.0%
		Final *wR*	4.1%
F(000)	1172	GOF*	1.42

Unit-cell contents $4\{[Mg_3[B_{11}O_{15}(OH)_6]\}$

$R = \Sigma(||F_o|-|F_c||)/\Sigma|F_o|$

$wR = [\Sigma w(|F_o|-|F_c|)^2/\Sigma wF_o^2]^{1/2}$, $w = 1/sig^2(F)$

* GOF = Goodness of fit

Infrared spectroscopy

A powdered sample was prepared by grinding by hand about 20 mg of preobrazhenskite in an alumina mortar until the grain size was generally less than 2 μm. About 4 mg of sample was mixed with 150 mg of KBr by grinding by hand in an alumina mortar. The resulting mixture was pressed in an evacuated die into a 13 mm pellet. A high-resolution infrared spectrum was recorded on a Bomen Michelson 100 Fourier-transform interferometric infrared spectrometer. Frequency measurements were calibrated internally against a He–Ne laser, and are accurate to 0.01 cm^{-1} according to the manufacturer.

Structure Refinement

Scattering curves for neutral atoms, together with anomalous dispersion corrections, were taken from Cromer & Mann (1968) and Cromer & Liberman (1970), respectively. The Siemens SHELXTL PLUS (PC version) system of programs was used throughout this study. *R* indices are of the form given in Table 1, and are given as percentages.

Refinement of the structure was done in the space group *Pbcn*, with the atomic coordinates of Rumanova *et al.* (1972) as the starting model. Refinement of the

TABLE 2. ATOMIC COORDINATES AND EQUIVALENT ISOTROPIC DISPLACEMENT PARAMETERS FOR PREOBRAZHENSKITE

	x	*y*	*z*	**U*$_{eq}$
Mg(1)	0	0.4283(1)	1/4	63(3)
Mg(2)	0.16602(4)	0.06238(8)	0.41426(7)	59(2)
B(1)	0	0.1388(3)	1/4	67(7)
B(2)	0.0888(1)	0.1852(2)	0.0696(2)	63(5)
B(3)	0.1038(1)	0.9591(2)	0.1976(2)	67(5)
B(4)	0.1012(1)	0.7022(2)	0.1200(2)	58(5)
B(5)	0.2122(1)	0.7785(2)	0.2614(2)	69(5)
B(6)	0.1721(1)	0.3557(2)	0.4096(2)	72(5)
O(1)	0.06782(8)	0.0493(1)	0.2943(1)	67(3)
O(2)	0.03051(9)	0.2389(1)	0.1497(1)	83(4)
OH(3)	0.1236(1)	0.2678(2)	-0.0231(2)	212(5)
O(4)	0.11387(9)	0.0420(2)	0.0758(1)	82(4)
O(5)	0.18564(9)	0.9202(1)	0.2493(1)	85(3)
OH(6)	0.05602(8)	0.8269(1)	0.1729(1)	69(3)
OH(7)	0.04590(9)	0.5744(2)	0.1171(1)	98(4)
O(8)	0.13128(9)	0.7432(2)	-0.0041(1)	69(3)
O(9)	0.17179(9)	0.6660(2)	0.2032(1)	77(3)
O(10)	0.28184(9)	0.7489(2)	0.3281(1)	90(4)
OH(11)	0.27252(9)	0.9609(2)	0.4745(1)	95(4)
OH(12)	0.38678(9)	0.9396(2)	0.3345(1)	101(4)
H(3)	0.126(2)	0.351(3)	-0.027(3)	150
H(6)	0	0.825(5)	1/4	150
H(7)	0.009(2)	0.609(3)	0.065(3)	150
H(11)	0.230(2)	0.434(3)	0.545(3)	150
H(12)	0.136(2)	0.488(4)	0.299(3)	150

*$U_{eq} = U_{eq} \times 10^4$

TABLE 3. ANISOTROPIC DISPLACEMENT PARAMETERS FOR PREOBRAZHENSKITE

	*U_{11}	U_{22}	U_{33}	U_{23}	U_{13}	U_{12}
Mg(1)	56(5)	55(5)	78(5)	0	3(3)	0
Mg(2)	60(3)	55(3)	62(3)	−1(3)	0(2)	4(2)
B(1)	73(12)	63(12)	64(12)	0	11(10)	0
B(2)	92(9)	72(9)	86(9)	7(7)	8(8)	−9(7)
B(3)	60(8)	76(9)	65(9)	2(7)	−7(7)	1(7)
B(4)	74(9)	42(8)	58(9)	−5(7)	0(7)	−2(7)
B(5)	83(9)	71(9)	55(9)	1(7)	7(7)	0(7)
B(6)	79(9)	65(9)	73(9)	−2(7)	21(7)	−7(7)
O(1)	67(6)	74(6)	61(6)	−7(5)	−4(5)	11(5)
O(2)	91(6)	61(6)	96(6)	17(5)	21(5)	0(5)
OH(3)	307(10)	105(6)	223(9)	57(7)	160(8)	24(7)
O(4)	100(6)	74(6)	74(6)	11(5)	28(5)	17(5)
O(5)	71(6)	67(6)	118(6)	−15(5)	−22(5)	7(5)
OH(6)	65(6)	58(6)	86(6)	−10(5)	19(5)	−5(5)
OH(7)	108(7)	89(7)	96(6)	19(5)	−32(5)	−35(5)
O(8)	79(6)	65(6)	62(6)	5(5)	21(5)	7(5)
O(9)	79(6)	66(6)	86(6)	11(5)	−26(5)	9(5)
O(10)	85(6)	76(6)	110(6)	−17(5)	−32(5)	6(5)
OH(11)	105(6)	102(6)	79(6)	15(5)	15(5)	41(5)
OH(12)	87(7)	95(7)	122(7)	53(6)	12(5)	14(5)

*$U_{ij} = U_{ij} \times 10^4$

positional parameters and an isotropic displacement model gave an R index of 6.0%. Conversion to an anisotropic displacement model, together with the refinement of all parameters, led to convergence to an R index of 4.6%. A three-dimensional difference-Fourier map was calculated, and the positions of all five hydrogen atoms were located. Refinement of all parameters, including the positional coordinates of the hydrogen atoms, gave a final R index of 4.0% and a wR index of 4.1%. Refinements using a structure-factor weighting scheme and an isotropic extinction correction were tried, but neither improved the results of the refinement. Final positional parameters and equivalent isotropic displacement parameters are given in Table 2, anisotropic displacement parameters in Table 3, selected interatomic distances and angles in Table 4, and a bond-valence analysis in Table 5. Observed and calculated structure-factors are available from the Depository of Unpublished Data, CISTI, National Research Council, Ottawa, Ontario K1A 0S2.

RESULTS

Fundamental building block

Only three borate mineral structures are known to have *FBB*s ($B_n\phi_m$, ϕ: unspecified anion) that contain more than six boron atoms; these occur in preobrazhenskite, with n = 9, and in the polymorphs

TABLE 4. SELECTED INTERATOMIC DISTANCES (Å) AND ANGLES (°) FOR PREOBRAZHENSKITE

Mg(1)–O(2),a	2.096(2) x2	B(3)–O(5)	1.484(3)
Mg(1)–OH(7),a	2.081(2) x2	B(3)–OH(6)	1.466(3)
Mg(1)–OH(12)b,c	2.052(2) x2	B(3)–O(1)g	1.441(3)
<Mg(1)–O>	2.076	B(3)–O(4)g	1.504(3)
		<B(3)–O>	1.474
Mg(2)–O(1)	2.045(2)		
Mg(2)–O(4)d	2.135(2)	B(4)–OH(6)	1.472(3)
Mg(2)–O(5)e	2.201(2)	B(4)–OH(7)	1.480(3)
Mg(2)–O(8)f	2.062(2)	B(4)–O(8)	1.460(3)
Mg(2)–O(10)c	2.117(2)	B(4)–O(9)	1.485(3)
Mg(2)–OH(11)e	2.070(2)	<B(4)–O>	1.472
<Mg(2)–O>	2.105		
		B(5)–O(5)	1.377(3)
B(1)–O(1),a	1.454(2) x2	B(5)–O(9)	1.371(3)
B(1)–O(2),a	1.489(2) x2	B(5)–O(10_	1.363(3)
<B(1)–O>	1.471	<B(5)–O>	1.370
B(2)–O(2)	1.365(3)	B(6)–O(8)f	1.448(3)
B(2)–OH(3)	1.362(3)	B(6)–O(10)c	1.506(3)
B(2)–O(4)	1.378(3)	B(6)–OH(11)c	1.489(3)
<B(2)–O>	1.368	B(6)–OH(12)c	1.464(3)
		<B(6)–O>	1.477
Hydrogen bonding			
OH(3)–H(3)	0.76(3)	H(3)···OH(11)h	2.39(3)
		H(3)···OH(12)i	2.43(3)
OH(3)···OH(11)h	3.012(2)	OH(3)–H(3)···OH(11)h	139(3)
OH(3)···OH(12)i	3.084(2)	OH(3)–H(3)···OH(12)i	145(3)
OH(6)–H(6)	1.224(2)	H(6)···OH(6)e	1.224(2)
OH(6)···OH(6)e	2.447(3)	OH(6)–H(6)···OH(6)e	178(4)
OH(7)–H(7)	0.87(3)	H(7)···OH(3)e	2.48(3)
OH(7)···OH(3)e	3.273(3)	OH7–H(7)···OH(3)e	152(2)
OH(11)–H(11)	0.79(3)	H(11)···O(9)f	2.13(3)
OH(11)···O(9)f	2.833(2)	OH(11)–H(11)···O(9)f	148(3)
OH(12)–H(12)	0.69(3)	H(12)···O(9)	2.01(3)
OH(12)···O(9)	2.675(2)	OH(12)–H(12)···O(9)	163(3)
Mg(1) octahedron			
O(2)–O(2)a	2.341(3)	O(2)–Mg(1)–O(2)a	67.9(1)
O(2),a–OH(7),a	3.109(2) x2	O(2),a–Mg(1)–OH(7),a	96.2(1)
O(2),a–OH(12)b,c	3.057(2) x2	O(2),a–Mg(1)–OH(12)b,c	92.0(1)
O(2),a–OH(12)b,c	2.984(2) x2	O(2),a–Mg(1)–OH(12)b,c	92.6(1)
OH(7)–OH(7)a	3.183(3)	OH(7)–Mg(1)–OH(7)a	99.7(1)
OH(7),a–OH(12)b,c	2.918(2) x2	OH(7),a–Mg(1)–OH(12)b,c	88.8(1)
OH(7),a–OH(12)b,c	2.831(2) x2	OH(7),a–Mg(1)–OH(12)b,c	86.5(1)
<O–O>	2.943	<O–Mg(1)–O>	90.2
Mg(2) octahedron			
O(1)–O(4)d	3.182(2)	O(1)–Mg(2)–O(4)d	99.1(1)
O(1)–O(8)e	2.305(2)	O(1)–Mg(2)–O(5)e	85.6(1)
O(1)–O(8)f	3.040(2)	O(1)–Mg(2)–O(8)f	95.5(1)
O(1)–O(10)c	3.080(2)	O(1)–Mg(2)–O(10)c	95.4(1)
O(4)d–O(5)e	3.661(2)	O(4)d–Mg(2)–O(5)e	116.2(1)
O(4)d–O(8)f	2.884(2)	O(4)d–Mg(2)–O(8)f	86.8(1)
O(4)d–OH(11)e	2.798(2)	O(4)d–Mg(2)–OH(11)e	83.4(1)
O(5)e–O(10)c	3.175(2)	O(5)e–Mg(2)–O(10)c	94.6(1)
O(5)e–OH(11)e	2.795(2)	O(5)e–Mg(2)–OH(11)e	81.7(1)
O(8)f–O(10)c	2.271(2)	O(8)f–Mg(2)–O(10)c	85.8(1)
O(8)f–OH(11)e	3.567(2)	O(8)f–Mg(2)–OH(11)e	119.4(1)
O(10)c–OH(11)e	3.169(2)	O(10)c–Mg(2)–OH(11)e	99.2(1)
<O–O>	2.996	<O–Mg(2)–O>	91.8
B(1) tetrahedron			
O(1)–O(1)a	2.400(3)	O(1)–B(1)–O(1)a	111.2(2)
O(1),a–O(2),a	2.439(2) x2	O(1),a–B(1)–O(2),a	111.9(1)
O(1),a–O(2),a	2.395(2) x2	O(1),a–B(1)–O(2),a	108.9(1)
O(2)–O(2)a	2.341(3)	O(2)–B(1)–O(2)a	103.7(2)
<O–O>	2.401	<O–B(1)–O>	109.4
B(2) triangle			
O(2)–OH(3)	2.389(2)	O(2)–B(2)–OH(3)	122.3(2)
O(2)–O(4)	2.392(2)	O(2)–B(2)–O(4)	121.4(2)
OH(3)–O(4)	2.327(2)	OH(3)–B(2)–O(4)	116.2(2)
<O–O>	2.369	<O–B(2)–O>	120.0

TABLE 4. continued

B(3) tetrahedron			
O(5)–OH(6)	2.418(2)	O(5)–B(3)–OH(6)	110.1(2)
O(5)–O(1)g	2.305(2)	O(5)–B(3)–O(1)g	104.0(2)
O(5)–O(4)g	2.445(2)	O(5)–B(3)–O(4)g	109.8(2)
OH(6)–O(1)g	2.419(2)	OH(6)–B(3)–O(1)g	112.7(2)
OH(6)–O(4)g	2.417(2)	OH(6)–B(3)–O(4)g	108.9(2)
O(1)g–O(4)g	2.429(2)	O(1)g–B(3)–O(4)g	111.1(2)
<O–O>	2.406	<O–B(3)–O>	109.4
B(4) tetrahedron			
OH(6)–OH(7)	2.398(2)	OH(6)–B(4)–OH(7)	108.7(2)
OH(6)–O(8)	2.365(2)	OH(6)–B(4)–O(8)	108.1(2)
OH(6)–O(9)	2.417(2)	OH(6)–B(4)–O(9)	109.6(2)
OH(7)–O(8)	2.445(2)	OH(7)–B(4)–O(8)	113.2(2)
OH(7)–O(9)	2.396(2)	OH(7)–B(4)–O(9)	107.8(2)
O(8)–O(9)	2.396(2)	O(8)–B(4)–O(9)	109.4(2)
<O–O>	2.403	<O–B(4)–O>	109.5
B(5) triangle			
O(5)–O(9)	2.395(2)	O(5)–B(5)–O(9)	121.3(2)
O(5)–O(10)	2.372(2)	O(5)–B(5)–O(10)	119.8(2)
O(9)–O(10)	2.353(2)	O(9)–B(5)–O(10)	118.8(2)
<O–O>	2.373	<O–B(5)–O>	120.0
B(6) tetrahedron			
O(8)f–O(10)c	2.271(2)	O(8)f–B(6)–O(10)c	100.4(2)
O(8)f–OH(11)c	2.453(2)	O(8)f–B(6)–OH(11)c	113.3(2)
O(8)f–OH(12)c	2.411(2)	O(8)f–B(6)–OH(12)c	111.8(2)
O(10)c–OH(11)c	2.491(2)	O(10)c–B(6)–OH(11)c	112.5(2)
O(10)c–OH(12)c	2.448(2)	O(10)c–B(6)–OH(12)c	111.0(2)
OH(11)c–OH(12)c	2.386(2)	O(11)c–B(6)–OH(12)c	107.8(2)
<O–O>	2.410	<O–B(6)–O>	109.5

a = $\bar{x}$, y, ½–z; b = x–½, y+½, ½–z; c = ½–x, y–½, z; d = x, $\bar{y}$, ½+z; e = x, y–1, z; f = x, 1–y, z+½; g = x, y+1, z; h = ½–x, y–½, z–½; i = ½–x, ½–y+1, z–½

pringleite and ruitenbergite, with $n = 12$ (Grice *et al.* 1994). The *FBB* of preobrazhenskite (Fig. 1) contains four symmetrically distinct boron positions. The B(1) position is tetrahedrally coordinated and sits on a two-fold axis at the center of the *FBB*. The $B(1)O_4$ tetrahedron, with a <B–O> distance of 1.471 Å, shares its ligands with two B(2) triangles and two B(3) tetrahedra. The B(2) triangles and B(3) tetrahedra also share a ligand, forming three-membered rings (Fig. 1). The $B(2)O_2(OH)$ triangle has a <B–O> distance of 1.368 Å, and the $B(3)O_3(OH)$ tetrahedron has a <B–O> distance of 1.474 Å, values within the ranges typically observed for $<^{[3]}B–O>$ and $<^{[4]}B–O>$. Each of the B(3) tetrahedra share ligands with a B(4) tetrahedron and a B(5) triangle; the B(4) tetrahedron and B(5) triangle also share a ligand, again forming two three-membered rings (Fig. 1). The $B(4)O_2(OH)_2$ tetrahedron and the $B(5)O_3$ triangle have <B–O> distances of 1.472 and 1.370 Å, respectively.

The *FBB* of preobrazhenskite contains four three-membered boron–oxygen rings, each of which contain two tetrahedra and one triangle (Fig. 1). The *FBB* is decorated at each end by the addition of $B(6)O_2(OH)_2$ tetrahedra, with a <B–O> distance of 1.477 Å, which shares a single ligand with the B(5) triangle (Fig. 1). Using the notation of Christ & Clark (1977), this *FBB* block may be written as $9:(4\Delta + 5T) + 2T$.

The *FBB* contains a short OH(6)–OH(6) distance [2.447(3) Å], which suggests a hydrogen bond between ligands of the same *FBB*. Examination of the difference-Fourier map in that region clearly shows a

TABLE 5. BOND-VALENCE* ANALYSIS (v.u.) FOR PREOBRAZHENSKITE

	Mg(1)	Mg(2)	B(1)	B(2)	B(3)	B(4)	B(5)	B(6)	H(3)	H(6)	H(7)	H(11)
O(1)		0.386	$0.799^{x2}\downarrow$		0.828							
O(2)	$0.336^{x2}\downarrow$		$0.727^{x2}\downarrow$	1.016								
OH(3)				1.025					0.8		0.2	
O(4)		0.303		0.981	0.698							
O(5)		0.253			0.737		0.984					
OH(6)					0.774	0.761				$0.5^{x2}\downarrow$		
OH(7)	$0.350^{x2}\downarrow$					0.745					0.8	
O(8)		0.369				0.808		0.812				
O(9)						0.735	1.000					0.2
O(10)		0.318					1.022	0.694				
OH(11)		0.361						0.727	0.1			0.8
OH(12)	$0.379^{x2}\downarrow$							0.778	0.1			
Σ	2.130	1.990	3.052	3.022	3.037	3.049	3.006	3.011	1.0	1.0	1.0	1.0

* parameters from Brown & Altermatt (1985)

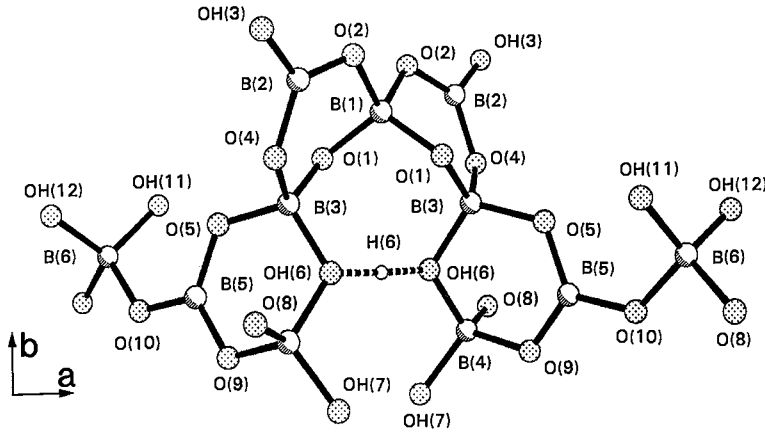

FIG. 1. The fundamental building block in preobrazhenskite.

hydrogen atom on the two-fold axis halfway between the symmetry-related OH(6) positions (Fig. 1). The question of a symmetrical hydrogen-bond is addressed below.

Mg octahedra

The preobrazhenskite structure contains two symmetrically distinct Mg positions. The Mg(1) position occurs on a two-fold axis and is octahedrally coordinated by 2 O^{2-} and 4 OH^- ligands, with a <Mg–O> distance of 2.076 Å; individual Mg(1)–O distances range from 2.052 to 2.096 Å. The Mg(2) site is octahedrally coordinated by 5 O^{2-} and 1 OH^- ligands. This octahedron is significantly distorted, with a <Mg–O> distance of 2.105 Å and a range of Mg(2)–O distances

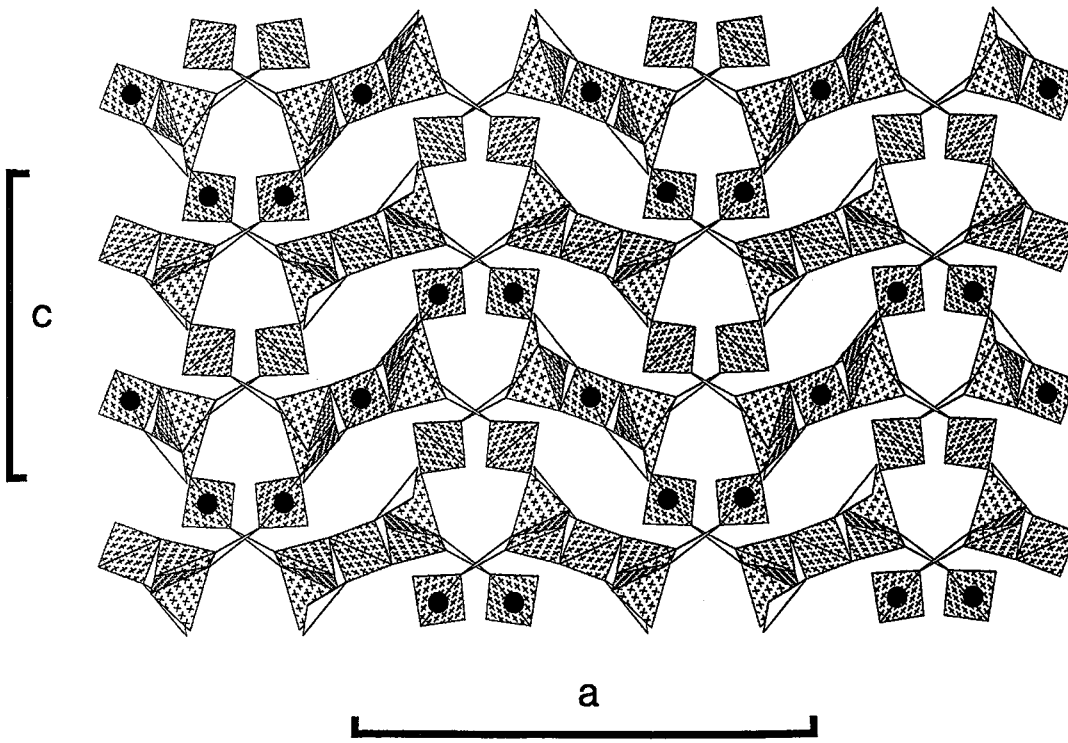

FIG. 2. The structure of preobrazhenskite projected onto (010). Borate tetrahedra are shaded with crosses, borate triangles are given as open triangles, and magnesium positions are shown as solid circles.

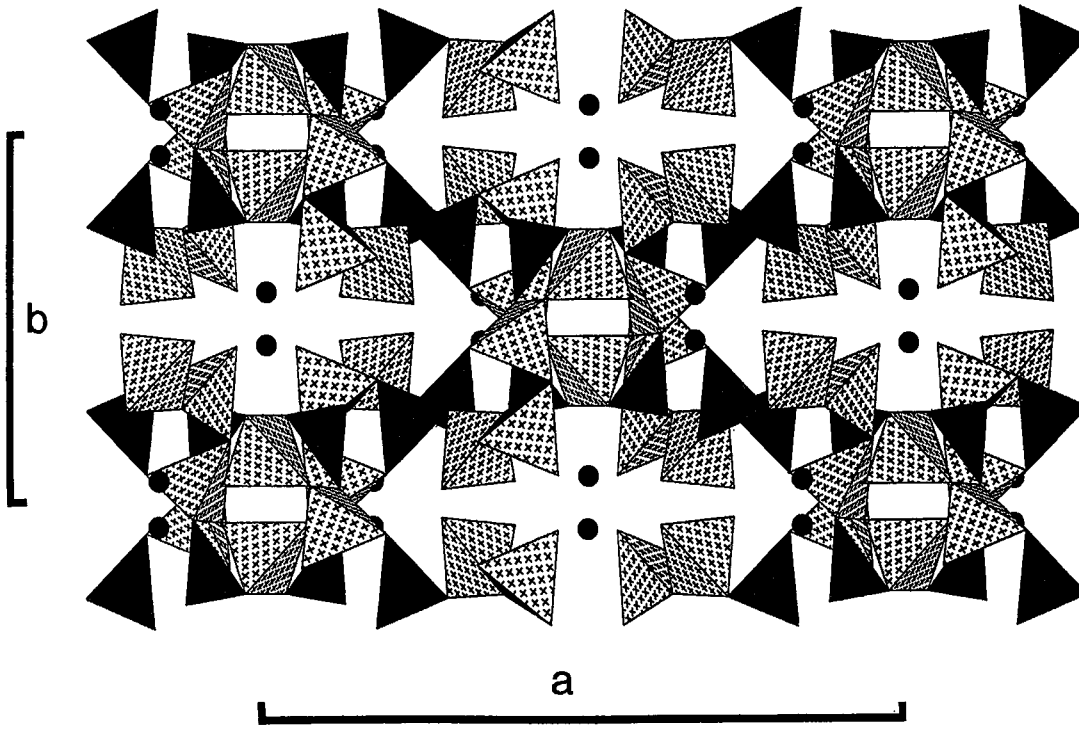

FIG. 3. The structure of preobrazhenskite projected onto (001). Borate tetrahedra are shaded with crosses, borate triangles are given as solid triangles, and magnesium positions are shown as solid circles.

between 2.045 and 2.201 Å.

Borate sheets

The borate *FBB* (Fig. 1) shares its O(8) ligands with four adjacent *FBB*s to form complex sheets parallel to (010). There are two such sheets per unit cell. They are offset, and the lower sheet has its B(2) triangles pointing upward (as in Fig. 1), whereas the upper sheet has its B(2) triangles pointing downward (Fig. 2). The Mg(1) and Mg(2) positions are sandwiched between the borate sheets (Fig. 3), and each ligand of each octahedron is also part of the borate sheets. Together with hydrogen bonding, Mg provides the intersheet linkage. The resulting structure is tightly bonded in all directions, explaining why preobrazhenskite has a hardness of 5 and no cleavage.

Hydrogen bonding

The hydrogen positions obtained *via* least-squares refinement of the X-ray data are realistic in terms of bond lengths and angles (Table 4), as well as the bond-valence requirements of the donor and acceptor anions (Table 5). Hydrogen bonds play three structural roles in preobrazhenskite: (1) they bridge between anions of the *same FBB*, (2) they bridge between anions of the *same* borate sheet, but of *different FBB*s, (3) they bridge between anions of *adjacent* borate sheets.

The OH(6) position is shared between the B(3) and

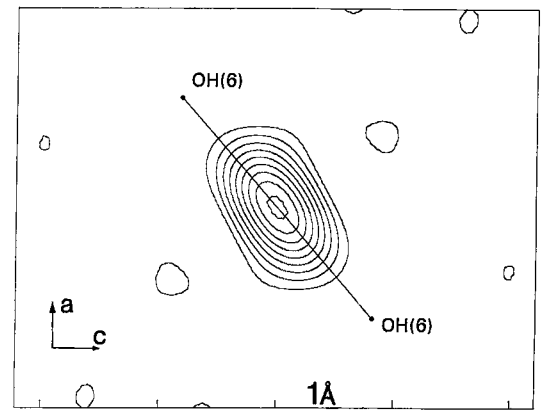

FIG. 4. Difference-Fourier map of the H(6) position calculated with the H(6) position vacant. Contour interval is 0.1 $e/Å^3$

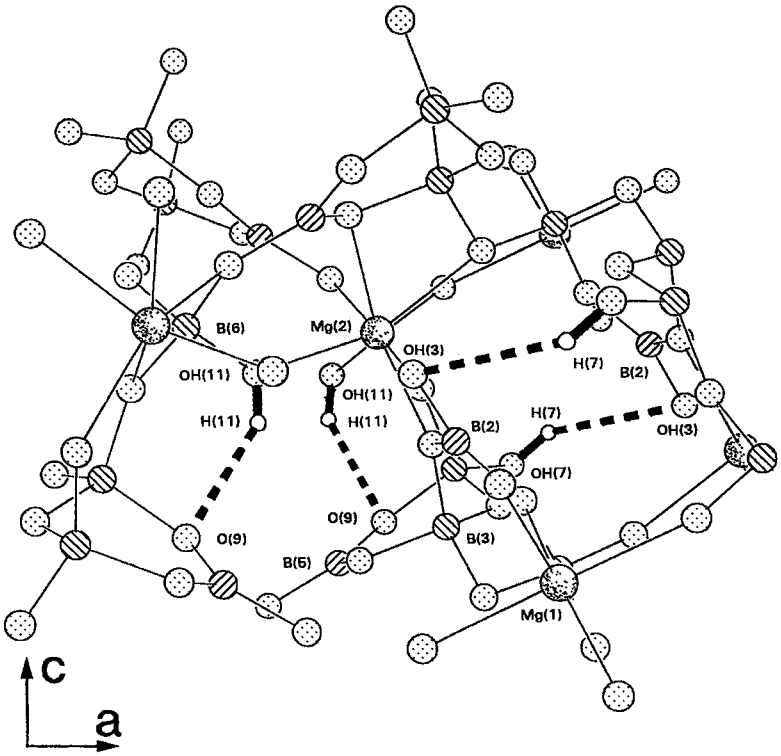

FIG. 5. The structure of preobrazhenskite projected onto (010). Boron atoms are shaded with parallel lines, oxygen atoms, with regular dots, magnesium atoms, with a random dot pattern, and hydrogen atoms are given as small open circles. Hydrogen bonds are shown as heavy solid and dashed lines.

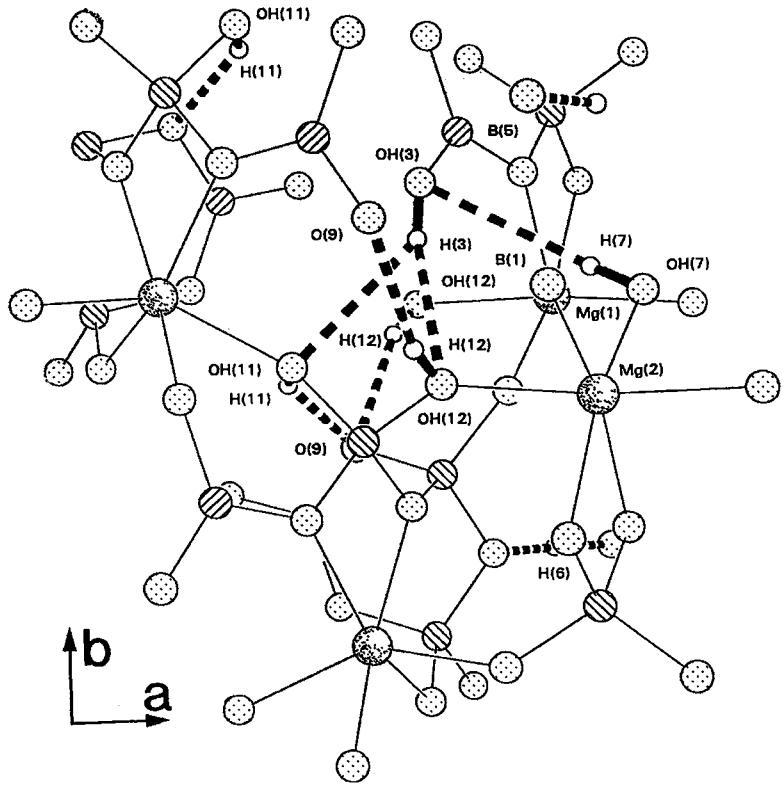

FIG. 6. The structure of preobrazhenskite projected onto (001). Legend as in Fig. 5.

B(4) tetrahedra, which contribute 1.53 *v.u.* towards satisfying its bond-valence requirements. This position is not compatible with an OH(6)–H(6) bond-length of ~0.9 Å, as this would contribute an additional 0.8 *v.u.* to the OH(6) position, giving an unrealistic total of 2.33 *v.u.* However, the OH(6) position is related to the OH(6)a position *in the same FBB* through the two-fold rotational axis, with an OH(6)–OH(6)a distance of 2.447(3) Å, compatible with a hydrogen bond. A difference-Fourier map, calculated with the H(6) position vacant, clearly shows the presence of the H(6) atom on the two-fold axis halfway between the two OH(6) positions (Fig. 4). This symmetrical hydrogen bond gives OH(6)–H(6) and H(6)–OH(6)a distances of 1.224(2) Å, with a bond-valence of 0.5 contributed to each OH(6) position, giving bond-valence totals of 2.035 *v.u.* per OH(6). Note that the OH(6)–H(6)–OH(6)a bond involves elements of the same *FBB* (Fig. 1).

The OH(11)–H(11)...O(9)f bond links two adjacent *FBB*s in the same borate sheet (Fig. 5). This bond is relatively strong, with a H(11)...O(9)f distance of 2.13(3) Å, and provides additional rigidity to the borate sheets.

The OH(7)–H(7)...O(3)e and OH(12)–H(12)...O(9) bonds bridge adjacent borate sheets (Figs. 5, 6) and provide additional intersheet bonding. The H(3) position also bonds adjacent sheets, but there are two possible acceptor anions. The OH(3)–H(3)...OH(11)h and OH(3)–H(3)...OH(12)i configurations have acceptor distances of 2.39(3) and 2.43(3) Å, respectively, and each bond involves a reasonable OH(3)–H(3)...OH bond-angle (Table 4). Bond-valence arguments (Table 5) support both of these anions as acceptors for the hydrogen bond. The OH(3) anisotropic displacement parameters (Table 3) are three times larger than the average for the other anions. This indicates positional disorder at the OH(3) site, and suggests that there may be two local configurations, *i.e.*, OH(3)′–H(6)′–OH(11)h and OH(3)″–H(6)″–OH(12)i, where the OH(3)′–OH(3)″ separation is less than the resolution of the X rays.

Infrared spectrum

The powder infrared spectrum of preobrazhenskite (Fig. 7) in the principal OH-stretching region shows three prominent peaks between 3700 and 3000 cm^{-1}; in addition, there is a prominent shoulder and a barely resolved shoulder to the high-frequency side of the high-frequency band. Band positions and intensities are given in Table 6.

There are five distinct hydrogen-positions in preobrazhenskite (Table 2), and the bands of Table 6 will correspond to the five distinct (OH) groups in the structure, as there is no cation disorder that could give rise to fine structure in this region. The spectrum was fitted by optimization and least-squares techniques to five bands (Fig. 7, Table 6). We found *empirically* that the peak shape was best described by a Pearson func-

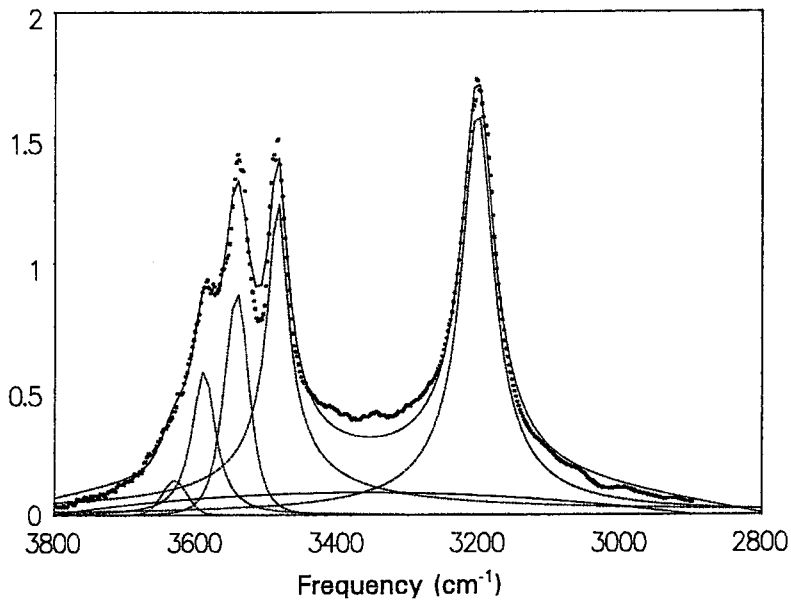

FIG. 7. The infrared spectrum of preobrazhenskite in the principal OH-stretching region.

TABLE 6. BAND POSITIONS AND INTENSITIES IN THE PRINCIPAL OH-STRETCHING REGION OF PREOBRAZHENSKITE

Band	Position	Intensity	Assignment	Σbv.* at acceptor
A	3204	163.1	H(6)	1.535
B	3485	131.4	H(7)	1.825
C	3544	44.1	H(3)	1.922
D	3590	33.4	H(11)	1.935
E	3631	6.3	H(12)	1.935

* the bond-valence sum (Σbv.) is the total bond velence at the acceptor anion less the contribution due to the hydrogen bond.

tion. There are some unsatisfactory characteristics to the fit; it is obvious that a skew (nonsymmetrical) function would better describe the band shape, but (at the moment) the solution is adequate to describe the principal features of the spectrum. The problem of peak shape will be addressed in a later, more extensive study of the infrared spectra of borate minerals.

The frequency of the principal OH-stretching band is a function of the strength of the hydrogen bond, lower frequencies being characteristic of stronger hydrogen bonds. We may assess the strengths of the hydrogen bonds in the structure of preobrazhenskite from the incident bond-valence sums at the acceptor anions (ignoring the contribution of the incident hydrogen-bonds); these values are given in Table 6. Figure 8 shows that the band frequency is a linear function of the bond-valence deficiency at the acceptor anion. The *A* band at 3203 cm^{-1} is of particular interest. This has a very low frequency for an OH band, similar to that observed in other structures in which a hydrogen atom is (ideally) halfway between

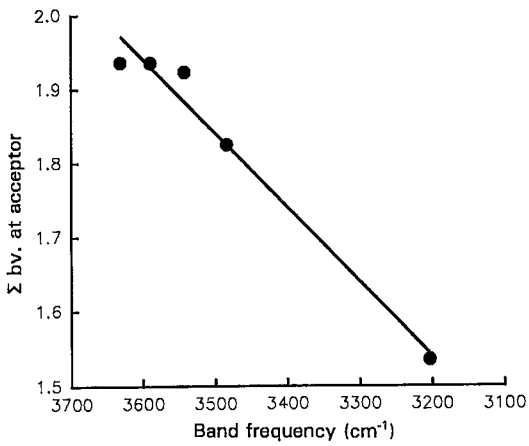

FIG. 8. Band frequency in the OH-stretching region as a function of bond-valence sum (Σbv.) at the acceptor anion in preobrazhenskite.

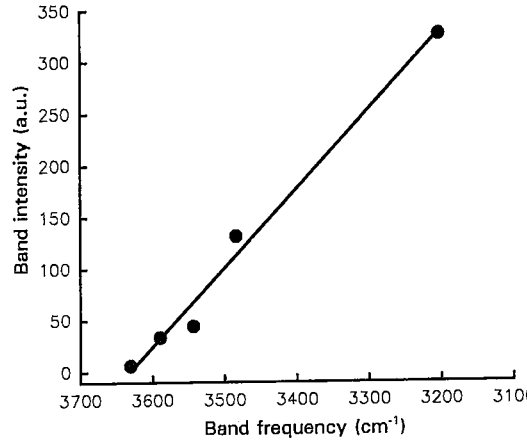

FIG. 9. Band intensity (arbitrary units; corrected for H-atom multiplicity) as a function of band frequency in the OH-stretching region of preobrazhenskite.

two symmetrically equivalent anions (*e.g.*, vesuvianite; Groat *et al.* 1995). The question of whether or not a symmetrical hydrogen-bond occurs in this (and other) structures is somewhat moot. If the hydrogen atom assumes a disordered, off-center arrangement at room temperature, there is the possibility that it assumes a symmetrical configuration at higher temperatures, with the ensuing ferroelectric phase transition.

The variation in band intensity as a function of frequency is of considerable interest here. Figure 9 shows this variation for the bonds in preobrazhenskite; the band intensities have been corrected for the differences in (OH) multiplicity. This shows that the intensity of the band is strongly a function of bond energy (as well as the amount of H in the structure contributing to that band). Similar results have been found by Skogby & Rossman (1991) on single-crystal spectra of amphiboles in the OH-stretching region. This feature is not well characterized in minerals, and extensive further work on the spectroscopy of borate minerals is planned.

ACKNOWLEDGEMENTS

This work was supported by the Natural Sciences and Engineering Research Council of Canada *via* Operating, Equipment and Infrastructure grants to FCH, and by a Killam Fellowship to FCH. The University of Manitoba supported this work with a Postgraduate Fellowship to PCB and the J.S. Lightcap Fellowship to PCB. The reviews of two anonymous referees, and editorial work by Dr. R.F. Martin, improved the clarity and quality of this contribution.

REFERENCES

BROWN, I.D. & ALTERMATT, D. (1985): Bond-valence parameters obtained from a systematic analysis of the inorganic structure database. *Acta Crystallogr.* **B41**, 244-247.

CHRIST, C.L. & CLARK, J.R. (1977): A crystal-chemical classification of borate structures with emphasis on hydrated borates. *Phys. Chem. Minerals* **2**, 59-87.

CLARK, J.R. & CHRIST, C.L. (1977): Unusual hydrogen bonding in some hydrated borate structures. *Acta Crystallogr.* **B33**, 3272-3273.

CROMER, D.T. & LIBERMAN, D. (1970): Relativistic calculation of anomalous scattering factors for X rays. *J. Chem. Phys.* **53**, 1891-1898.

_____ & MANN, J.B. (1968): X-ray scattering factors computed from numerical Hartree–Fock wave functions. *Acta Crystallogr.* **A24**, 321-324.

GRICE, J.D., BURNS, P.C. & HAWTHORNE, F.C. (1994): Determination of the megastructures of the borate polymorphs pringleite and ruitenbergite. *Can. Mineral.* **32**, 1-14.

GROAT, L.A., HAWTHORNE, F.C., ROSSMAN, G.R. & ERCIT, T.S. (1995): The infrared spectroscopy of vesuvianite in the OH region. *Can. Mineral.* **33** (in press).

RUMANOVA, I.M., RAZMONOVA, Z.P. & BELOV, N.V. (1972): Crystal structure of preobrazhenskite $3MgO{\cdot}5.5B_2O_3{\cdot}4.5H_2O = Mg_3[B_{11}O_{14}(OH)_8HO_2]$. *Sov. Phys. Dokl.* **16**, 518-521.

SKOGBY, H. & ROSSMAN, G.R. (1991): The intensity of amphibole OH bands in the infrared absorption spectrum. *Phys. Chem. Minerals* **18**, 64-68.

YARZHEMSKII, YA.YA. (1956): Preobrazhenskite, a new borate mineral of the salt deposits of the Inder dome. *Dokl. Akad. Nauk SSSR* **111**, 1087-1090 (in Russ.).

Received May 21, 1993, revised manuscript accepted September 20, 1993.